Colloid Polym Sci (2004) 282: 957–964
DOI 10.1007/s00396-003-1017-8

ORIGINAL CONTRIBUTION

América Vázquez-Olmos
David Díaz
Geonel Rodríguez-Gattorno
José Manuel Saniger-Blesa

Activation of CdS nanoparticles by metallic ions and their selective interactions with PAMAM dendrimers

Received: 18 August 2003
Accepted: 16 October 2003
Published online: 18 December 2003

A. Vázquez-Olmos (✉)
J.M. Saniger-Blesa
Centro de Ciencias Aplicadas y Desarrollo Tecnológico, Universidad Nacional Autónoma de México, Ciudad Universitaria, D. F. 04510, México
E-mail: amer@aleph.cinstrum.unam.mx

D. Díaz · G. Rodríguez-Gattorno
Facultad de Química, Universidad Nacional Autónoma de México, Ciudad Universitaria, D. F. 04510, México

Abstract CdS nanoparticles (NPs) in colloidal dispersion were activated by metallic ions [Mn(II) and Cu(II)], employing a simple method under mild conditions. These metallic ions on the surface of the CdS NPs quench the red-shifted defect emission, and efficiently promote near band gap emission; they also enhance the photo stability and dispersability of the suspensions. Taking advantage of the chemical affinity of Mn(II) and Cu(II) for the CdS surface, we carried out a study of the interaction between [CdS-M(II)$_n$] NPs and polyamidoamine dendrimers of 1 and 2.5 generations ($G_1 = 8$ amino, and $G_{2.5} = 32$ carboxylic end-groups, respectively). The strong interaction between these two chemical species results in the formation of new [CdS-M(II)$_n$ G$_n$] nanocomposites. All colloidal systems were monitored by UV-visible electronic absorption and emission spectroscopies, and electronic paramagnetic resonance. The crystal structures of the nanocomposites, as well as their average diameters (2.0–3.3 nm), were determined by high-resolution transmission electron microscopy images.

Keywords CdS nanoparticles · Nanocomposites · Dendrimers · Surface modification

Introduction

The large surface area of a nanoparticle (NP) and its immediate environment, such as capping agents and solvent molecules, have strong effects on the particle properties. For example, depending on the surface modifier nature, it is possible to modify the charge, functionality, and reactivity and enhance the stability and dispersability, in comparison with the naked NPs. Optical, magnetic, or catalytic properties may be also readily imparted to the dispersed colloidal NPs [1]. Nanocomposites (NCs) often exhibit improved physical and chemical properties over their single-component counterparts [2, 3, 4, 5, 6, 7], which results in a broader range of applications. The above-mentioned is very important if we consider the effort that has been directed to the design and controlled fabrication of nanostructured materials with functional properties in recent years [8, 9, 10, 11, 12, 13]. Moreover, the synthesis of NCs in colloidal dispersions is also of interest from fundamental and academic points of view, in areas such as colloid and interface science.

In a previous work, we reported a method to prepare CdS NPs with a narrow size distribution, which involves the use of the relatively labile capping agents 2-ethylhexanoate anion (ethex) and dimethyl sulfoxide (DMSO) [4]. We found that these two surface modifiers are in constant dynamic exchange between adsorbed and dissolved conditions and that they can therefore be easily replaced with other chemical species. As a matter of fact, starting from [CdS(ethex)$_n$] NPs colloidal dispersions in DMSO, we carried out in a simple way, under mild reaction conditions, the surface substitution of the ethex anions by metallic cations. In this work we present the synthesis of such [CdS-M(II)$_n$] NPs, as well as the effect of Mn(II) and Cu(II) on the optical behaviors, stabilities and dispersabilities of the resulting colloids.

In addition, due to the chemical affinity of the dendrimers' end-groups toward the divalent cations on the CdS NPs surface, included in this paper is a study of the interaction of the polyamidoamine (PAMAM) dendrimers of low generation (Fig. 1) G_1 (8 amino end-groups) and $G_{2.5}$ (32 carboxyl end-groups), with [CdS-Cu(II)$_n$] and [CdS-Mn(II)$_n$] NPs, respectively, in colloidal dispersions.

PAMAM dendrimers are extremely regular and highly branched organic polymers, which have different reaction sites including their interior and periphery. The external surface of PAMAM dendrimers may end with amino groups, producing the so-called full generations or, with carboxylate groups, producing the so-called half-generations [14, 15]. From computer assisted molecular modeling, it has been found that above generation 4, the PAMAM dendrimers are spherical, but below this generation they have hemispherical dome shapes [14, 16]. Furthermore, due to the singular chemical and structural properties of dendrimers, a large number of potential applications have been suggested [17, 18, 19, 20, 21].

All the colloidal systems were characterized by UV-visible electronic absorption, and emission spectroscopies, electronic paramagnetic resonance (EPR) and high-resolution transmission electron microscopy (HR-TEM). This being a long-term spectral study, the behavior of all the dispersions was followed by absorption and emission spectroscopies over several months and during this time we observed no flocculation in any case.

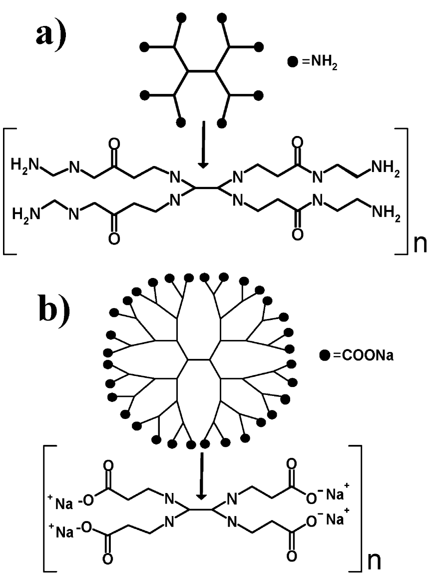

Fig. 1a, b Simplified representation of **a** G_1 polyamidoamine (PAMAM) dendrimer, and **b** $G_{2.5}$ PAMAM dendrimer. The corresponding general representation of whole and half generations is in *brackets*. Based on their structures, the diameters of G_1 and $G_{2.5}$ PAMAM dendrimers have been estimated around 2.16 and 3.56 nm, respectively [19]

Materials and methods

Materials Cadmium 2-ethylhexanoate [Cd(ethex)$_2$] (from Strem), sodium sulfide (*Ultra puris*, Fluka), $CuCl_2{\cdot}2H_2O$ (97%, Baker), $MnCl_2{\cdot}4H_2O$ (98.7%, Baker), DMSO (99.9%, Aldrich), methanol (MeOH) (99.9%, Merck), G_1 and $G_{2.5}$ starburst PAMAM dendrimers (Aldrich) and N_2 gas (Praxair, 99.999%) were used in their commercial forms. Ultra-pure water (18 MΩ) was obtained from a Barnsted E-pure deionization system.

Synthesis procedure [CdS(ethex)$_n$] NPs were synthesized according to the procedure previously reported in [4]. A $2{\times}10^{-4}$ M Cd(ethex)$_2$ solution (25 ml) in DMSO, previously purged with nitrogen for 30 min (in order to remove trace amounts of oxygen), was sonicated for 15 min and then 0.10 ml of $1{\times}10^{-2}$ M aqueous Na_2S solution was rapidly injected into the vigorously stirred Cd^{2+} solution. The subsequent ripening process of the CdS dispersions took place within about 2 weeks. If the colloids are stored in darkness, their UV-visible absorption spectral profile does not change in several months. A high purity of Na_2S and a low concentration of cadmium ions are important factors in producing CdS nanocrystallites with a narrow size distribution.

The preparation of CdS NPs activated with Cu^{2+}, [CdS-Cu(II)$_n$] or Mn^{2+}, [CdS-Mn(II)$_n$], was carried out by rapid mixing of 5 ml of a fresh [CdS(ethex)$_n$] dispersion with 5 ml of a $2{\times}10^{-4}$ M $CuCl_2{\cdot}2H_2O$ solution in DMSO, or 5 ml of a $2{\times}10^{-4}$ M $MnCl_2{\cdot}4H_2O$ solution in MeOH, under N_2 atmosphere and stirring for 25 min. Based on the manufacturer's value of the dendrimer weight fractions in MeOH, as well as the known dendrimer densities, we prepared $2{\times}10^{-4}$ M dendrimer stock solutions in DMSO (previously N_2-bubbled for 30 min).

Colloids of CdS NPs activated with divalent metals, [CdS-M(II)$_n$] and PAMAM dendrimers [CdS-M(II)$_n$]G_n (where $G_n = G_1$ or $G_{2.5}$), were prepared by mixing 5 ml of a fresh $2{\times}10^{-4}$ M G_n solution in DMSO, with 5 ml of the fresh [CdS-M(II)$_n$] colloidal dispersion, with stirring for 30 min. All colloidal dispersions were stored in darkness at room temperature. The systems presented in this paper were prepared in triplicate and the results were always reproducible. We did not observe any flocculation of the colloids studied.

Instruments UV-visible absorption spectra were obtained using an HP84–52A diode array Hewlett-Packard spectrophotometer. Fluorescence spectra were collected on a Fluoromax SPEX spectrofluorometer. The 200 mesh copper grids were coated with a layer of carbon. A drop of colloidal DMSO dispersion was deposited onto a copper grid, and the solvent evaporated under vacuum. These samples were analyzed by HR-TEM, using a JEOL 4000 EX instrument, operating at 400 kV. The size distribution was obtained from a digitalized amplified micrograph by averaging the larger and smaller axis diameters measured for each particle. The EPR spectra were recorded on a Bruker ED 200 equipment, in X-band frequency, at 77 K.

Results and discussion

Freshly synthesized colloidal dispersions of [CdS(ethex)$_n$] NPs in DMSO, showed an UV-visible absorption

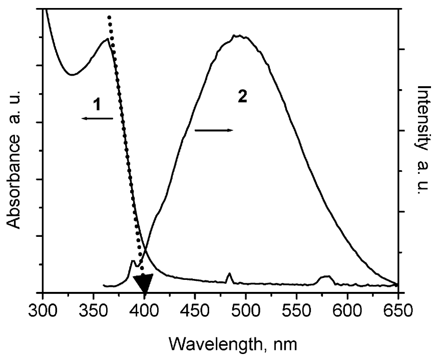

Fig. 2 Absorption (*1*) and emission (*2*) spectra of a colloidal dispersion of [CdS(ethex)$_n$] nanoparticles in DMSO (λ_{ex} = 350 nm), after storage in a light-protected environment for two weeks. The *dotted line* shows the intersection of the tangent with the wavelength axis for the absorption spectrum

spectrum with a maximum at 349 nm, characteristic of the first excitonic transition. Two weeks later, the maximum was observed at 364 nm (Fig. 2), but the spectrum did not change further in several months. The band gap energy of semiconductor NPs can be estimated from the absorption edge value (obtained from the intersection of the tangent with the wavelength axis). Due to size quantum effects, the first excitonic transition (or band gap) increases in energy as the particle diameter decreases [22, 23, 24]. This has been confirmed experimentally for a wide range of semiconductor nanocrystallites [4, 8, 9, 10].

An average diameter of 3.4 nm for the [CdS(ethex)$_n$] nanoclusters was estimated from the absorption edge value of 402 nm (3.1 eV) (see Fig. 2), using Brus's effective mass model [24]. The emission spectrum of these [CdS(ethex)$_n$] colloidal dispersions, obtained with an excitation wavelength of 350 nm (Fig. 2), displayed a broad emission band with a maximum at 492 nm, and $\Delta\lambda_{1/2}$ = 129.5 nm. This broad emission band is commonly attributed to the recombination of charge carriers immobilized in traps of different energies.

Activation of CdS NPs by M(II) ions

As mentioned previously, the surface modifiers (ethex anions) bind to CdS NPs in a non-covalent form; they are in a constant dynamic exchange between adsorbed and dissolved conditions. Sometimes, they can be easily replaced by other chemical species, such as the $[MoS_4]^{-2}$ ion, a very strong Lewis base [25]. However, the replacement of the ethex anions by M(II) ions (Mn^{2+} or Cu^{2+}) on the CdS NPs surfaces, under mild conditions, is a slow process.

In the case of [CdS-Mn(II)$_n$] NPs, the electronic absorption spectrum, immediately after mixing [CdS(ethex)$_n$] and Mn(II) (Fig. 3a), displayed a weak, broad band centered at 390 nm, which disappeared with time; on the other hand, a new absorption band appeared at 284 nm after 1 month; the intensity of this band increased substantially with time, and 6 months later, a maximum at 274 nm was observed. However, no further spectral changes were registered, at least within a year (Fig. 3a). The very significant shift toward higher energies observed can be attributed to the confinement of charge carriers, as a result of the CdS NPs' size decrease when the ethex anions are substituted for Mn^{2+} cations on the surface, driving the formation of [CdS-Mn(II)$_n$] NPs. An average diameter of 2.20 nm was estimated for these particles from the corresponding absorption edge value of 301 nm (4.1 eV), using Brus's model.

The emission spectrum (λ_{ex} = 266 nm) of this [CdS-Mn(II)$_n$] colloidal dispersion, recorded 1 month after its preparation (Fig. 3b), showed an intense and narrow

Fig. 3 **a** UV-visible absorption spectra of [CdS(ethex)$_n$] NPs in DMSO (*1*), 2×10^{-4} M $MnCl_2.4H_2O$ solution in MeOH (*2*), [CdS(ethex)$_n$] NPs colloids immediately after mixing with the Mn^{2+} solution (*3*), after 1 month (*4*), and 6 months later (*5*). **b** Emission spectra of [CdS-Mn(II)$_n$] NPs (λ_{ex} = 266 nm), after 1 month (*1*) and 6 months later (*2*). **c** X-band electronic paramagnetic resonance (EPR) spectrum of [CdS-Mn(II)$_n$] in 1:1 DMSO:MeOH, at 77 K (center field in 3480 Gauss, power = 0.632 mW). *Allowed transitions (Δm_I = 0), Δ forbidden transitions ($\Delta m_I \neq 0$)

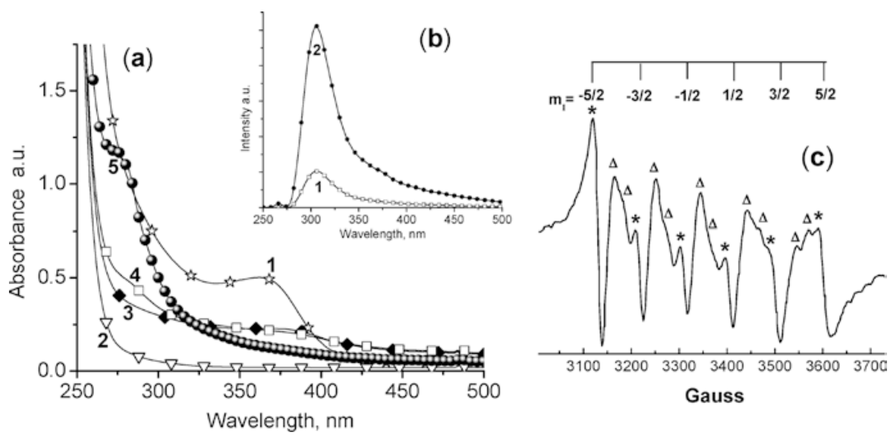

peak at $\lambda_{max} = 306$ nm, which was fivefold enhanced 5 months later. This behavior can be understood in terms of a substantial reorganization of the emitting states, promoted by surface-bound Mn(II). Therefore, in the activated $[CdSMn(II)_n]$ NPs, the appearance of a near band gap emission band becomes the predominant process of electron-hole recombination due to the severe decrease of traps. A similar CdS photoactivation by Cd^{2+} was observed by Henglein and co-workers in 1987 [2].

If we consider that the Mn(II) ions on the outside diffuse into the nanocrystallite lattice, or if these ions became buried in the inside as the nanocluster aggregated and grew, we might expect an ultraviolet emission decrease and the appearance of an orange emission, originated from the ${}^6A_1 \leftarrow {}^4T_1$ transition ($\lambda_{max} \sim 585$ nm) in Mn^{2+} [26, 27, 28]. Nevertheless, this behavior was not observed.

The oxidation state of the manganese on the surface of the CdS NPs was corroborated by EPR. The X-band frequency EPR spectrum of $[CdS\text{-}Mn(II)_n]$ NPs in 1:1 DMSO:MeOH, at 77 K was obtained 6 months after their preparation (Fig. 3c). We observed the typical signal of Mn^{2+} in a glassy matrix, characterized by a doublet of lines between the main lines, due to the so-called forbidden transitions ($\Delta m_I \neq 0$) [29]. The spectroscopic ground state of Mn(II) is ${}^6S$, with total spin $S = 5/2$ and nuclear spin $I = 5/2$, that gives rise to the usual sextet of main lines in the EPR spectra. The calculated g value is 2.005 and the hyperfine coupling constant is $A = 87.05 \times 10^{-4}$ cm^{-1}. The presence of forbidden transitions indicates that the Mn^{2+} ions do not occupy the cubic sites in the CdS core NPs, because purely cubic centers have zero probability for forbidden transitions [30, 31]. Thus, the hyperfine-structure spectrum further evidence that the manganese ions are on surface sites of the CdS NPs.

A similar behavior to that of the Mn^{2+}-activated CdS nanoclusters was observed when Cu^{2+} was added to pre-formed $[CdS(ethex)_n]$ nanoclusters in DMSO. The electronic absorption spectrum, immediately after mixing the $[CdS(ethex)_n]$ colloidal dispersions with Cu(II) (Fig. 4a), showed a band with a maximum at 298 nm. The absorption edge and maximum shifted toward higher energies with time (Fig. 4a). Even after 8 months, the absorption spectrum of the $[CdS\text{-}Cu(II)_n]$ NPs dispersions showed a band with $\lambda_{max} = 276$ nm and an absorption edge value of 334 nm (3.7 eV); from the latter value, Brus's model predicts an average diameter of 2.3 nm for these NPs. When the $[CdS\text{-}Cu(II)_n]$ colloidal dispersion was irradiated with 270 nm light, an emission band with a maximum at 317 nm, was observed after 1 month (Fig. 4b). After 8 months, this emission band shifted slightly to 308 nm, and was ca. seven times more intense.

It has been suggested that when Cu^{2+} replaces Cd^{2+} ions in the CdS lattice, a new, red-shifted emission peak appears, due to a new surface state whose energy lies into the semiconductor band gap. For example, in CdS crystals ("ultrahigh purity"; 1–2 mm thick) doped with Cu^{2+}, the cation produces two discrete surface-state levels at $E_c = -1.2$ eV and at $E_v = +2.3$ eV [32]. In films, the band-gap energy of undoped CdS changes from 2.48 eV (close to the corresponding value for single crystalline CdS of 2.53 eV) to 2.3 eV after Cu doping, resulting in a mid-gap state [33].

In our case, we have not observed any red-shifted emission peaks and neither have we observed absorption bands characteristic of d - d transitions corresponding to macro-crystalline Cu(II) coordination compounds. Besides, DMSO solutions of $CuCl_2$ and $Cu(ethex)_2$, with the same final concentration, do not fluoresce.

Fig. 4 a UV-visible absorption spectra of $[CdS(ethex)_n]$ dispersions in DMSO (*1*), 2×10^{-4} M $CuCl_2.2H_2O$ solution in DMSO (*2*), CdS colloids immediately after mixing with Cu(II) (*3*), after 1 month (*4*), and 8 months later (*5*). **b** Emission spectra of $[CdS\text{-}Cu(II)_n]$ NPs colloidal dispersions ($\lambda_{ex} = 270$ nm) after 1 month (*1*), and 8 months later (*2*). **c** X-band EPR characteristic spectrum of $[CdS\text{-}Cu(II)_n]$ nanocomposites (NCs) in DMSO, recorded at 77 K (center field in 3500 Gauss, power = 0.632 mW)

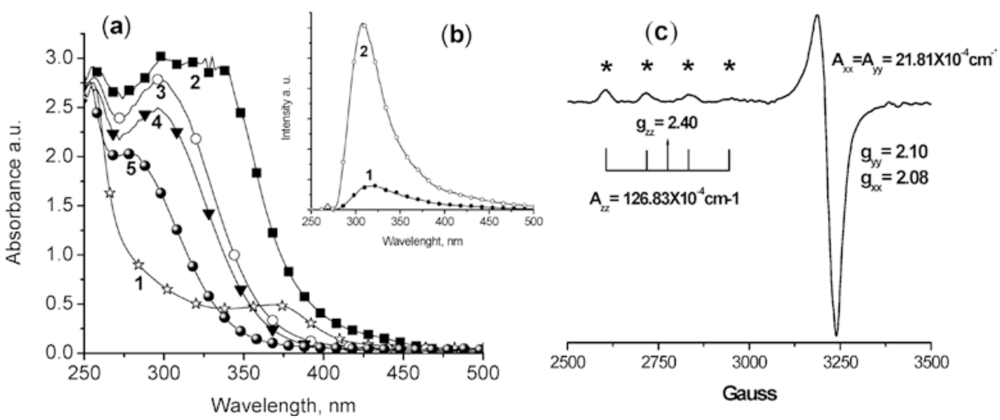

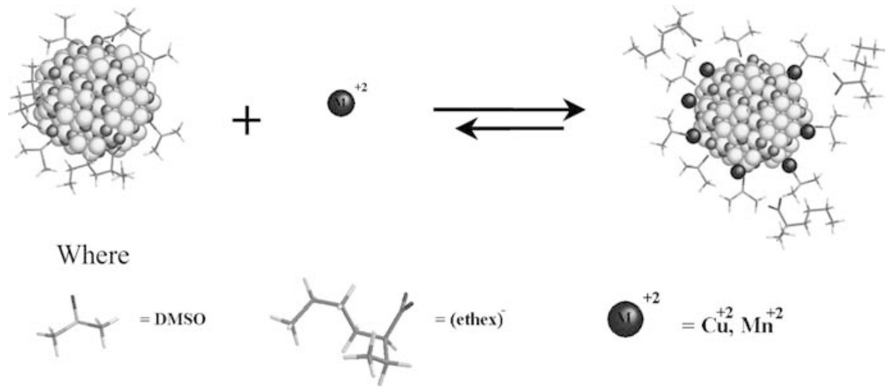

Fig. 5 Schematic representation of [CdS(ethex)$_n$] NPs and their surface modification by metal cations

X-band frequency EPR spectra of [CdS-Cu(II)$_n$] NPs in DMSO, at 77 K, were recorded at different points (Fig. 4c). The spectroscopic ground state of Cu(II) is ^2S, with total spin $S = 1/2$ and nuclear spin $I = 3/2$, giving rise to the usual quadruplet in the EPR spectra [29]. The signal characteristic of Cu^{2+} in a glassy matrix, with an elongated octahedral structure and an almost axial symmetry, where g_{zz} (2.40) > g_{xx} (2.08)≈ g_{yy} (2.10) was always observed.

On the basis of the previously discussed results, we may suggest that the colloidal dispersions of [CdS-M(II)$_n$] NPs [M = Mn(II) or Cu(II)] studied display the same general behavior. That is, in both cases, the formation of small NPs ($d \approx$2.20 nm) is favored when the metallic ions slowly replace the ethex anions on the CdS surface (Fig. 5). It is very important to remember that the Cu(II) and Mn(II) salts were added to freshly prepared [CdS(ethex)$_n$] colloidal dispersions, i.e. when the majority of the NPs must have been small-sized.

Furthermore, surface modification of CdS NPs with Mn(II) and Cu(II), quenches the red-shifted defect emission and efficiently promotes near band gap emission (Fig. 6). Additionally, it leads to an enhancement of their photo-stability and dispersability. Even though some papers concerning the activation of CdS NPs with Cu(II) [5, 34] have been published, none of such colloidal systems exhibited the same optical properties of those obtained in this work, in view of the different preparation conditions, and, of course, the different molecular surroundings.

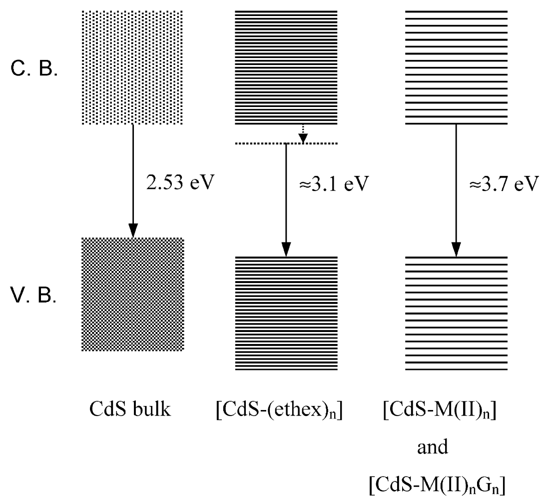

Fig. 6 Schematic energy level diagram of CdS NCs, showing the effect of ethex anions, M(II) cations, and their interaction with G_n PAMAM dendrimers, on the electronic states. The energy values for all the nanospecies were computed from the corresponding UV-visible electronic absorption spectra, using Brus's equation

Interactions of G_1 and $G_{2.5}$ PAMAM dendrimers with CdS NPs activated by Mn(II)

Mn(II) exhibits a great chemical affinity for oxygen donor Lewis bases, such as DMSO and the carboxylate end-groups of half generation PAMAM dendrimers [35, 36, 37]. Cu(II), on the other hand, although also able to interact with oxygen-donor ligands, has less affinity for oxygen than Mn(II); however, it displays a great tendency to bind to nitrogen-donor Lewis bases, including the end amino groups of whole generation PAMAM dendrimers. Therefore, on the basis of these considerations, we carried out a study of the interaction of G_1 (8-NH_2 end-groups) PAMAM dendrimers with [CdS-Cu(II)$_n$] NPs, as well as of $G_{2.5}$ (32-COO^- end-groups) PAMAM dendrimers with [CdS-Mn(II)$_n$] NCs.

[CdS-Mn(II)G2.5] spectra The absorption spectrum of $G_{2.5}$ dendrimers, in DMSO solution (Fig. 7a, spectrum 1), showed a band with a maximum around 284 nm, and a well-defined long-wave tail due to the fact that a whitish suspension was formed before mixing with the [CdS-Mn(II)$_n$] NPs. After this was done, the dispersion became clear and transparent within a few minutes. In Fig. 7a, spectrum 3, recorded 2 days later, showed a less defined long-wave tail, most likely due to the formation of $G_{2.5}$-DMSO aggregates. However, after 2 months, an

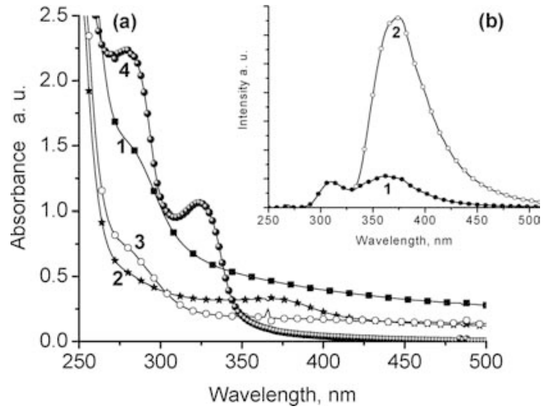

Fig. 7 **a** UV-visible absorption spectra of a 2×10^{-4} M $G_{2.5}$ PAMAM dendrimer solution in DMSO (*1*), CdS NPs immediately after mixing with Mn(II) (*2*), [CdS-Mn(II)$_n$] NPs 2 days after mixing with $G_{2.5}$ (*3*), and 2 months later (*4*). **b** Emission spectra of [CdS-Mn(II)$_n$] with $G_{2.5}$ PAMAM dendrimers after 2 months. *1* $\lambda_{ex}=270$ nm, *2* $\lambda_{ex}=315$ nm

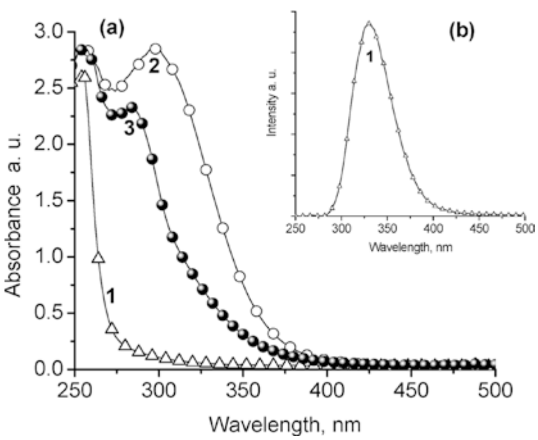

Fig. 8 **a** UV-visible absorption spectra of a 2×10^{-4} M G_1 PAMAM dendrimer solution in DMSO (*1*), [CdS-Cu(II)$_n$] NPs in DMSO (*2*), [CdS-Cu(II)$_n$] NPs after mixing with G_1 (*3*). **b** Emission spectrum of [CdS-Cu(II)$_n$ G_1] ($\lambda_{ex}=270$ nm), after mixing (*1*)

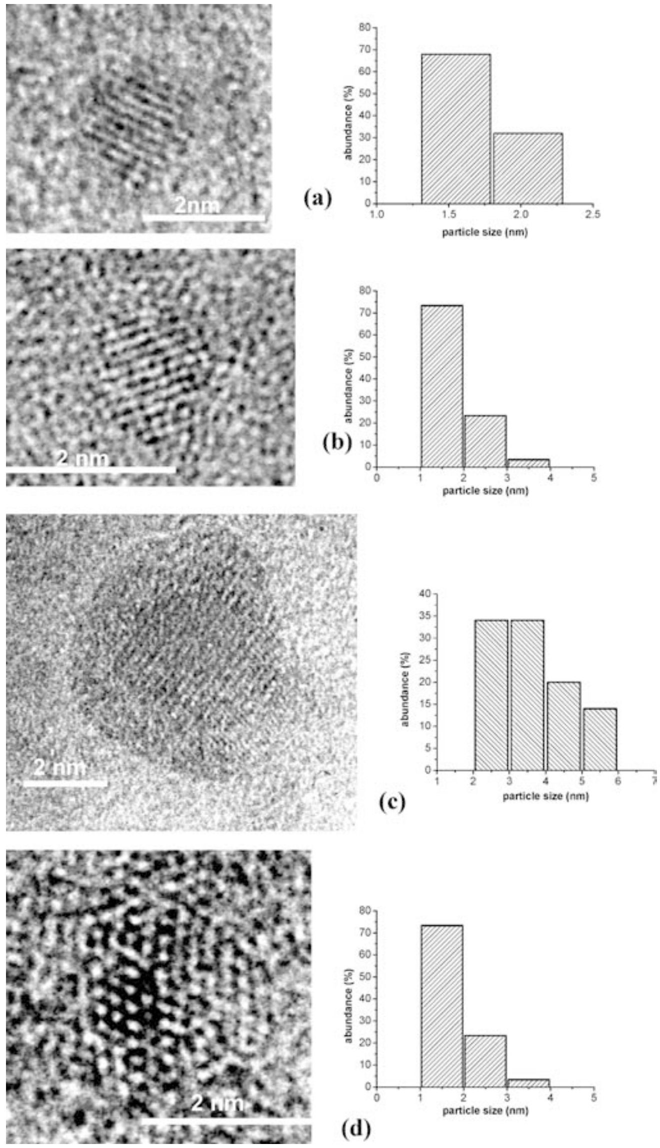

Fig. 9a–d Selected high-resolution transmission electron microscopy images of surface modified CdS NPs, and their corresponding histograms of particle size distributions. **a** [CdS-Mn(II)] nanoclusters ($d_{2,0,0}=2.85$ Å). **b** [CdS-Cu(II)] nanoclusters ($d_{3,1,1}=1.5$ Å). **c** [CdS-Mn(II)] with $G_{2.5}$ PAMAM dendrimers ($d_{2,2,0}=2.05$ Å). **d** [CdS-Cu(II)] with G_1 PAMAM dendrimers ($d_{2,2,0}=2.05$ Å)

intense absorption bimodal band was observed, with well-defined maxima at 280 nm and 326 nm (Fig. 7a, spectrum 4). It is possible to relate the latter to the coordination of the Mn(II) on the CdS NPs' surface to the carboxylate groups of the $G_{2..5}$ dendrimers, leading to the formation of new [CdS-Mn(II)$G_{2.5}$] NCs. Meanwhile, the first absorption band, centered at 280 nm, might be associated with remaining uncoordinated [CdS-Mn(II)$_n$] particles. Moreover, upon excitation with 270 nm light, the colloidal dispersion displayed two maxima at 310 nm and 365 nm (Fig. 7b). When an excitation wavelength of 315 nm was applied, a new emission band appeared at 370 nm, which was ca. six times more intense than those observed with $\lambda_{ex}=$ 270 nm.

EPR spectra of these dispersions were also collected, at 77 K in X-band frequency, which in all cases resulted very similarly to those shown in Fig. 3c. Therefore, it can be concluded that the oxidation state of the manganese has not been modified in the new NCs.

[CdS-Cu(II)G1] spectra When a fresh 2×10^{-4} M G_1 PAMAM dendrimer solution in DMSO was added to a [CdS-Cu(II)$_n$] colloidal dispersion, a colorless solution was produced, which displayed an absorption band with a maximum at 284 nm (Fig. 8a) and an absorption edge

Table 1 Summary of the spectral and HR-TEM results

Systems	Absorption edge (nm)	Band gap Eg (eV)[a]	ΔEg (eV)	Average cluster size (nm)[b]	Average cluster size (nm)[c]
CdS	402	3.1	0.6	3.4	–
[CdS-Mn(II)$_n$]	301	4.1	1.6	2.2	2.0 (SD = 0.2)
[CdS-Cu(II)$_n$]	334	3.7	1.2	2.3	2.0 (SD = 0.5)
[CdS-Mn(II)$_n$G$_{2.5}$]	348	3.6	1.1	2.7	3.3 (SD = 1.3)
[CdS-Cu(II)$_n$G$_1$]	329	3.8	1.3	2.4	2.2 (SD = 0.7)

[a]The band gap energy for CdS bulk is 2.53 eV [21]
[b]Calculated from the absorption edge, using Brus's effective mass model.
[c]Average diameter from HR-TEM micrographs, 50 particles measured.

value of 329 nm (3.8 eV). Brus's model predicts an average diameter of 2.4 nm for these NCs. The absorption spectrum remained unchanged for at least the next 4 months. The fresh [CdS-Cu(II)$_n$] colloidal dispersions did not have any significant emission upon excitation at 270 nm, but immediately after mixing with G$_1$ dendrimers, these new colloidal dispersions exhibited a strong and symmetric emission band, at 330 nm (Fig. 8b) with $\lambda_{1/2} = 51$ nm. Considering that the Cu^{2+} ions (bounded to the surface of the CdS NPs) show a great affinity to nitrogen atoms (of the amine moieties of the G$_1$ dendrimers, in this case), it is possible to suggest the formation of new [CdS-Cu(II)$_n$ G$_1$] NCs.

HR-TEM analysis The two stable crystalline phases of CdS are wurtzite (hexagonal) and zinc-blende (cubic), under normal reaction conditions. These polymorphs differ only in their second nearest neighbor arrangement. The primary surroundings and mass densities are identical, and the band gaps and optical reflectivity of the two phases are extremely close. It is well known that the aqueous precipitation of CdS can yield either the wurtzite or zinc-blende structure, depending on kinetic factors [38]. Direct measurements of the inter-planar spacing, from HR-TEM images of the previously discussed CdS colloidal systems, match the lattice spacing for cubic crystalline CdS particles. In Fig. 9, four selected HR-TEM images (and the corresponding particle size distribution) are presented, with $d_{h,k,l}$ lattice spacing for the CdS cubic structure: (a) [CdS-Mn(II)$_n$] NPs ($d_{2,0,0} = 2.85$ Å), (b) [CdS-Cu(II)$_n$] nanoclusters ($d_{3,1,1} = 1.5$ Å), (c) [CdS-Mn(II)] with G$_{2.5}$ PAMAM dendrimers ($d_{2,2,0} = 2.05$ Å), and (d) [CdS-Cu(II)] with G$_1$ PAMAM dendrimers ($d_{2,2,0} = 2.05$ Å). The average diameters directly measured from the HR-TEM micrographs for each system, agree well with those estimated from the UV-vis spectra. The comparison of these results is summarized in Table 1. From Fig. 9c, it can also be seen that some nanoclusters adopt a core-shell morphology, when the G$_{2.5}$ PAMAM dendrimers interact with [CdS-Mn(II)] nanoclusters.

In conclusion, the addition of Mn(II) or Cu(II) to the surface of pre-formed CdS nanoclusters dispersed in DMSO leads to the formation of long-time stable [CdS-M(II)$_n$] NPs, which are most likely to interact with a number of Lewis bases.

We have shown that the low generation PAMAM dendrimers have the capacity to tightly bind cation activated semiconductor nanoclusters, driving to the formation of [CdS-Mn(II)$_n$ G$_{2.5}$] and [CdS- Cu(II)$_n$ G$_1$] NCs. In summary, these metal ion-activated CdS NPs belong to a new generation of simple, relatively stable, paramagnetic and highly fluorescent species, quite convenient to react with a wide range of ligands for various purposes. [CdS-M(II)$_n$] NPs might be versatile units to auto-assemble through simple chemical procedures, in mild reaction conditions.

Acknowledgments This work was partially supported by UNAM-PAPIIT project no. IN107700. A. V.-O. is grateful to CTIC for a post-doctoral grant. We thank Mr. Luis Rendón-Vázquez (IF-UNAM) and Dr. Antonio Campero-Celis (UAM-I), for HR-TEM and EPR facilities and assistance, respectively. We also thank Dr. Silvia E. Castillo-Blum and Dr. Omar Jiménez-Sandoval for their valuable comments.

References

1. Caruso F (2001) Adv Mater 13:11
2. Spanhel L, Haase M, Weller H, Henglein A (1987) J Am Chem Soc 109:5649
3. Gehr RJ, Boyd RW, (1996) Chem Mater 8:1807
4. Díaz D, Rivera M, Ni T, Rodríguez J, Castillo-Blum SE, Nagesha D, Robles J, Álvarez-Fregoso OJ, Kotov NA (1999) J Phys Chem B 103:9854
5. Ni T, Nageshda DK, Robles J, Materer NF, Müssig S, Kotov NA (2002) J Chem Am Soc 124:3980
6. Dekany I, Nagy L, Turi L, Kiraly Z (1996) Langmuir 12:370
7. Dekany I, Turi L, Galbacs G, Fendler JH (1997) 213:584
8. Henglein A (1989) Chem Rev 89:1861
9. Weller H (1993) Angew Chem Int Edn Engl 32:41

10. Alivisatos AP (1996) J Phys Chem 100:13226
11. Norris DJ, Bawendi MG, Brus LE (1997) Mol Electron 281
12. Empedocles S, Bawendi M (1999) Acc Chem Res 32:389
13. Dekany I, Turi L, Galbacs G, Fendler JH (1999) J Colloid Interface Sci 213:584
14. Tomalia AD, Naylor A Del M, Goddard WA (1990) Angew Chem Int Edn Engl 29:138
15. Mekelburger HB, Jaworek W, Vögtle F (1992) Angew Chem Int Ed Engl 31:1571
16. Ardoin N, Astruc D (1995) Bull Soc Chim Fr 132:875
17. Tomalia DA (1995) Sci Am 272:42
18. Dvornic PR, Tomalia DA (1996) Curr Opinion Colloid Interface 1:221
19. Uppuluri S, Tomalia DA, Dvornic PR (1997) Polym Mater Sci Eng 77:116
20. Sooklal K, Hanus LH, Ploehn HJ, Murphy CJ (1998) Adv Mater 10:1083
21. Crooks RM, Zhao M, Sun L, Chechik V, Yeung L (2001) Acc Chem Res 34:181
22. Brus LE (1983) J Chem Phys 79:5566
23. Brus LE (1984) J Chem Phys 80:4403
24. Nedeljkovic JM, Patel RC, Kaufman P, Joyce-Pruden C, Leary NO (1993) J Chem Educ 70:342
25. Díaz D, Robles J, Ni T, Castillo-Blum SE, Nagesha D, Álvarez-Fregoso O J, Kotov NA (1999) J Phys Chem B 103:9859
26. Sooklal K, Cllum BS, Angel SM, Murphy CJ (1996) J Phys Chem 100:4551
27. Levy L, Feltin N, Ingert D, Pileni MP (1999) Langmuir 15:3386
28. Shu-Man L, Feng-Qi L, Hai-Quing G, Zhi-Hua Z, Zhan-Guo W (2000) Solid State Commun 115:615
29. Drago RS (1992) Physical methods. Saunders College Publishing, USA
30. Counio G, Esnouf T, Gacoin T, Boilot JT (1996) J Phys Chem 100:20021
31. Chen W, Sammynaiken R, Huang Y, Malm JO, Wallenberg R, Bovin JO, Zwiller V, Kotov NA (2001) J Appl Phys 89:1120
32. Rosenwaks Y, Burstein L, Shaphira Y, Huppert D (1990) J Phys Chem 94:6842
33. Petre D, Pintilie I, Pentia E, Botila T (1999) Mater Sci Eng B58 238
34. Isarov AV, Chrysochoos J (1997) Langmuir 13:3142
35. Cox PA (1989) The elements: their origin, abundance, and distribution. Oxford University Press, Oxford, UK
36. Calligaris M, Carugo O (1996) Coord Chem Rev 153:83
37. Elding LI (1996) Coord Chem Rev 153:1
38. Rossetti R, Ellison JL, Gibson JM, Brus LE (1984) J Chem Phys 80:4464